Control of the Electromechanical Properties of Alginate Hydrogels via Ionic and Covalent Cross-Linking and Microparticle Doping

Andrew D. Rouillard,[†] Yvonne Tsui,[‡] William J. Polacheck,[‡] Jae Youn Lee,[‡] Lawrence J. Bonassar,[§] and Brian J. Kirby*,[||]

Chemical and Biomolecular Engineering, Biological and Environmental Engineering, Biomedical Engineering, Mechanical and Aerospace Engineering, Cornell University, Ithaca, New York 14853

Received February 2, 2010
Revised Manuscript Received May 17, 2010

1. Introduction

Many tissues in the human body consist of cells embedded in an extracellular matrix that has an abundance of charged macromolecules. Examples of such tissues include tendon,[1] bone,[2] cartilage,[3−5] and corneal stroma.[6,7] Motions of the body impose on these tissues solid and fluid mechanical stimuli, such as compression, tension, and viscous shear due to fluid flow. Mechanical stimuli may influence cell behavior by activating cell signaling cascades that modulate gene expression or protein activity. Mechanical stimuli may act on cells directly (e.g., by perturbing stretch sensitive membrane proteins)[8,9] or indirectly through electric fields (e.g., by perturbing voltage-sensitive ion channels),[10−12] which are generated as a consequence of mechanical perturbation of the highly charged tissues. Understanding such mechanotransduction processes is important to enable design of tissue scaffolds that send appropriate regulatory signals to cells when mechanically stimulated.

In general, tissue engineering seeks (at the microscale) to mimic a cell's native chemical and mechanical environment and (at the macroscale) to mimic the function of tissue. Many macromolecular materials have been implemented for this purpose, including natural polymers such as chitosan,[13,14] alginate,[15,16] collagen,[17,18] and fibrin,[19] as well as synthetic polymers such as PEG-diacrylate[20,21] and PLGA.[22] Chemical biocompatibility is typically assessed in terms of binding, toxicity, degradability, and so on, and mechanical compatibility is assessed in terms of the similarity of the material's bulk mechanical properties to those of native tissue, as well as the material's ability to support phenotypic behavior, morphology, and gene expression.

While the chemical and mechanical properties of tissue scaffolds have received considerable attention, the electrical (and, in particular, electromechanical) properties of scaffolds have been less thoroughly explored. Descriptive work exists in native tissues, including detailed measurements and modeling of the electromechanics of cartilage[23−25] and bone.[26] Additionally, techniques have been investigated that use electrical stimulation to enhance healing of bone,[27] tendon,[28] and ligament.[29] However, the electromechanical properties of hydrogels remain largely unmeasured and have not been manipulated for tissue engineering applications.

Chondrocytes are an example of a cell type in which tissue-specific cell behavior has been observed to change as a function of electromechanical environment. Dynamic compression of cartilage tissue and chondrocyte-seeded tissue scaffolds stimulates chondrocytes to increase biosynthesis of glycosaminoglycans (GAG),[30,31] which are primarily responsible for the compressive strength of cartilage. Coupled mechanical, physicochemical, and electrical stimuli are thought to play a role in controlling chondrocyte response to mechanical loading.[31−37] In particular, the concentration of glycosaminoglycans in dynamically compressed samples is positively correlated with fluid velocity, indicating that the stimulus is related to fluid transport.[38,39] This points toward hydrodynamic shear, flow-enhanced nutrient transport, and flow-induced electric fields, which are all coupled to the intrinsic electromechanical properties of the tissue, as possible mechanotransduction stimuli. An understanding of the relative importance of these phenomena in regulating chondrocyte metabolism would be a significant achievement for cartilage tissue engineering and instruct better scaffold design.

The broad goal of this work is to develop materials with independently addressable chemical, mechanical, and electromechanical properties, such that the mechanotransduction of cells seeded into a hydrogel matrix can be separated into chemical, mechanical, and electrical responses. Of the available materials that have been used for 3D cell culture, including polyesters such as poly(lactic acid) and poly(glycolic acid);[22] natural polymers including collagen,[17] agarose,[40] chitosan,[13] alginate,[15] and fibrin;[19] and PEG-DA in native and modified form,[21,41,42] we selected alginate because it (a) is biodegradable with noninflammatory degradation products, (b) can be ionically or covalently cross-linked, (c) is inexpensive, and (d) has been used in numerous tissue engineering studies.

The immediate goal of this work is to investigate whether the electromechanical properties of alginate hydrogels can be independently varied using techniques compatible with seeding of primary cells.

2. Materials and Methods

Hydrogel Fabrication. *Ionic Cross-Linking.* The methods for generating ionically cross-linked alginate hydrogels were based on those used by Genes et al. for generating cell adhesive surfaces[43] and for chondrocyte encapsulation.[44,45] Alginate (Protanal LF1060, FMC Biopolymer) was dissolved in Dulbecco's phosphate-buffered saline (DPBS) with no calcium or magnesium (Mediatech) to make a 3% w/v alginate solution (note, throughout this paper, *X*% w/v = *X* g/100 mL). Calcium sulfate (Fisher Scientific) was mixed into DPBS to make a 3% w/v $CaSO_4$ solution (supersaturated). A total of 1 mL of the 3% w/v alginate solution and 0.5 mL of the 3% w/v $CaSO_4$ solution were each loaded into separate 3 mL syringes connected to a three-way stopcock. The alginate and calcium sulfate solutions were rapidly mixed by pumping the solutions between the syringes in three cycles.[46] The mixture was then ejected between two glass plates spaced 1 mm apart and allowed to gel for 5 min. The top glass plate was removed and the hydrogel slab was equilibrated in a solution of 10 mM 4-(2-hydroxyethyl)-1-piperazineethanesulfonic acid (HEPES, Mediatech), 150 mM NaCl (Sigma), and 15 mM $CaCl_2$ (Sigma) at pH 7.0 for at least 1 h before testing. After equilibration, the hydrogels decreased in volume by 1.5%, resulting in a final concentration of 2.0% w/v alginate. At the time of testing, 6 mm diameter discs were cut from the hydrogel slab with a biopsy punch.

* To whom correspondence should be addressed. Phone: 607-255-4379. E-mail: bk88@cornell.edu.
[†] Chemical and Biomolecular Engineering.
[‡] Biological and Environmental Engineering.
[§] Biomedical Engineering.
[||] Mechanical and Aerospace Engineering.

10.1021/bm1001312
Published on Web 07/21/2010

Covalent Cross-linking. A photo-cross-linking technique was used to make covalently cross-linked alginate hydrogels based on techniques reported by Smeds et al.[47] and Li et al.[48] This was motivated by a desire to eliminate divalent cations from the matrix. Photo-cross-linking was accomplished in a two-step process. First, anhydride chemistry was used to replace secondary alcohols on the alginate backbone with methacrylate groups in order to create methacrylate-alginate. Second, a solution of methacrylate-alginate was photo-cross-linked in the presence of a photoinitiator under exposure to ultraviolet light to initiate polymerization of the methacrylate groups, which formed the cross-links. The manuscript by Smeds et al. contains a description of the chemical structure of alginate before and after functionalization.[47]

Alginate (0.5 g) was dissolved into 20 mL of DI H_2O (Labconco) to make a 2.5% w/v alginate solution, and 20 mL of methacrylic anhydride (Alfa Aesar) was added to the solution. Base was added to improve the efficiency of the reaction via one of two techniques. In the first technique, which was used for the viability study, 5 M NaOH was added dropwise over 72 h to reach a total volume of 40 mL added.[47] In the second technique, which was later found to be more convenient, 3.5 mL of triethylamine (Sigma) was added concertedly to the solution.[49] In both cases, the mixture was covered to minimize evaporation and continuously stirred in a fume hood for 72 h. After the three day reaction period, the mixture was poured into 100 mL of ethanol (Sigma) to precipitate the methacrylate-alginate product. The mixture was vacuum filtered in a Buchner funnel through 5 μm filter paper. The product was recovered still wet and redissolved in 20 mL of DI H_2O, then precipitated, and filtered a second time. The methacrylate-alginate was then spread over a glass dish and allowed to dry in a fume hood for 24 h.

Methacrylate-alginate was dissolved in DPBS to make a 3% w/v alginate solution for photo-cross-linking. The photoinitiator VA-086 (Wako) was selected from a group of five photoinitiators that were tested for both photo-cross-linking performance and cytotoxicity over a range of photoinitiator concentrations and UV exposure times.[54] VA-086 was dissolved in 70% v/v ethanol to make a 10% w/v VA-086 solution. A total of 30 μL of the 10% w/v VA-086 solution was added to 1 mL of the 3% w/v alginate solution to make a 3% w/v alginate, 0.3% w/v VA-086 solution. The solution was poured between two glass plates spaced 1 mm apart. The mold was placed in the center of a UV oven (Spectroline) and exposed to 5 min of UV light (365 nm longwave, 2 μW/cm^2) to form covalent cross-links of the methacrylate groups on the alginate polymer chains. UV irradiation causes dissociation of the nitrogen−nitrogen double bond of the azo initiator VA-086, leading to the formation of photodissociated radicals that induce free-radical chain polymerization.[50] The top glass plate was removed and the hydrogel slab was placed in a solution of 10 mM HEPES and 150 mM NaCl at pH 7.0 for at least 1 h before testing. During equilibration, the hydrogels swelled 135% in volume, resulting in a final alginate concentration of 1.3% w/v. At the time of testing, 6 mm diameter discs were prepared with a biopsy punch.

Microparticle Doping. Ionically and covalently cross-linked hydrogels were doped with silica microparticles (Polygosil, Macherey-Nagel) by mixing silica into the alginate solutions at a concentration of 7% w/v silica prior to cross-linking. Silica particles had measured zeta potentials (Zetasizer, Malvern) of -8 ± 3 and -30 ± 5 mV in equilibration solutions with and without 15 mM Ca^{2+}, respectively. The silica-doped hydrogels were equilibrated as described for the undoped hydrogels prior to mechanical testing. Dilution during the fabrication processes resulted in a final concentration of 4.7% and 3.0% w/v for ionically and covalently cross-linked hydrogels, respectively. The silica particles had an average diameter of 5 μm with an average pore size of 6 nm and BET measured surface area of 400 m^2/g, as reported by the manufacturer.

Hydrogel Characterization. Hydrogel discs were characterized under uniaxial compression in a radially confined geometry using a mechanical tester (ELF 3100, Bose), confinement chamber outfitted with Ag/AgCl electrodes (Warner Instruments; Figure 1), and a bathing

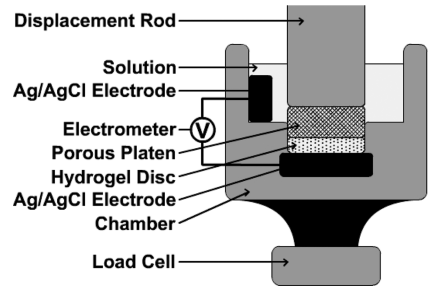

Figure 1. Testing apparatus for uniaxial compression in a radially confined geometry. Actuation of the displacement rod compresses the hydrogel disk. Fluid squeezed out of the hydrogel escapes through the porous polyethylene platen. Stress is registered by the load cell. Streaming potentials are measured by electrodes placed on opposite sides of the hydrogel disk.

solution of 10 mM HEPES and 150 mM NaCl at pH 7.0. Stress relaxation and dynamic compression tests were conducted in order to measure the stress (σ) and streaming potential (ΔV) signals generated by the hydrogels in response to applied strains. The data was fit to models from poroelastic theory[51−53] to calculate the aggregate (equilibrium) modulus (H_A), permeability (k), and electrokinetic coupling coefficient (K_e) of the hydrogels.

Stress Relaxation. Hydrogel discs were compressed in 5% increments at 3 min intervals up to 30% strain. Each step resulted in a stress spike and an ensuing decay as fluid and solid equilibrated in the disk. The decay in stress after each step was fit to the exponential function,

$$\sigma = \sigma_o e^{-t/\tau} + \sigma_{eq} \tag{1}$$

using nonlinear least-squares regression in order to determine the equilibrium stress (σ_{eq}) and time constant (τ) of the decay.[51] Equilibrium stress was plotted versus strain (ε) and fit to the second order polynomial,

$$\sigma_{eq} = c_1\varepsilon^2 + c_2\varepsilon \tag{2}$$

using nonlinear least-squares regression. Aggregate modulus,

$$H_A = \frac{d\sigma_{eq}}{d\varepsilon} \tag{3}$$

which is the equilibrium modulus obtained from uniaxial confined compression, was reported at 30% strain by evaluating the slope of the stress−strain curve.[51] The permeability,

$$k = \frac{\delta\delta_{eq}}{\pi^2 H_A \tau} \tag{4}$$

(also reported at 30% strain) was then calculated from the aggregate modulus, relaxation time constant, and disk thickness (δ).[51] The permeability is a proportionality constant that relates pressure gradient to fluid velocity and, thus, is a measure of the ease at which fluid can travel through a poroelastic material.

Dynamic Compression. Hydrogel discs were compressed sinusoidally at a 1% strain amplitude superimposed on a 30% static strain at a frequency of 1 Hz for 10 min. The dynamic stress response was computed from the force signal measured by a 1000 g load cell (Model 31 Mid, Honeywell Sensotec). The dynamic streaming potential was measured using a high impedance (2×10^{14} Ω) electrometer (Model 6514, Keithley) to record the potential across the Ag/AgCl electrodes located on either side of the hydrogel. The stress, strain, and streaming

potential signals were Fourier transformed to filter noise and compute the signal amplitudes and phase separations. Total harmonic distortion of the stress and streaming potential signals (i.e., power in the overtones divided by total power) were also monitored and were less than 10% for all reported experiments.

The streaming potential, as measured by the Ag/AgCl electrodes across the hydrogel, is generated by the convective flow of mobile counterions of the fixed charge in the hydrogel. The electrokinetic coupling constant was computed as the ratio of the streaming potential amplitude to the stress amplitude. For these materials at 1 Hz, this ratio becomes independent of frequency and is a very good approximation of the electrokinetic coupling constant. The dynamic streaming potential and electrokinetic coupling coefficient are indicators of the magnitude of the electrical response of the hydrogel relative to the mechanical response: fluid velocity and dynamic stress, respectively.

Dynamic compression data was also taken while sweeping the frequency (f) of oscillation from 0.001 to 10 Hz for at least 5 cycles at each frequency. The frequency response of the stress signal was fit to a model for the dynamic electromechanical behavior of cartilage[53]

$$\sigma = \frac{\Lambda_s u_o H_A \gamma \coth(\gamma\delta)}{\Lambda_s + \delta_{eq} H_A \gamma \coth(\gamma\delta)} \tag{5}$$

which gave the stress as a function of the platen stiffness (Λ_s), the strain amplitude (u_o), and a complex parameter γ, where

$$\gamma = \sqrt{\frac{i2\pi f}{H_A k}} \tag{6}$$

The aggregate (equilibrium) modulus H_A and the permeability k were determined by the fit, independent of the stress relaxation measurements. The complex parameter γ represents the reciprocal distance through which a displacement will propagate via fluid flow over the time f^{-1}, and delineates the transition from the "fluid dynamic" regime ($\gamma^{-1} > \delta$), in which fluid flow is able to dissipate stresses throughout the material, and the "fluid static regime" ($\gamma^{-1} < \delta$), in which fluid flow dissipates little stress. As indicated by eq 6, the permeability (which incorporates the relaxation time), determines the characteristic distance γ^{-1} for a particular frequency.

Viability Assay. Cartilage was harvested from the femoral condyles and femoropatellar groove of recently slaughtered calves. Large pieces of dissected cartilage were placed in a bath of DPBS with 1% v/v antibiotics and antimycotics (AB/AM, Mediatech, 10,000 IU/ml penicillin, 10 mg/mL streptomycin, 25 μg/mL amphotericin) at 37 °C. Harvested cartilage was cut into small 0.5 cm sized pieces, rinsed in DPBS with 1% v/v AB/AM, and placed into a solution of Dulbecco's modified Eagle's medium with 4.5 g/L glucose and L-glutamine and without sodium pyruvate (DMEM, Mediatech) with 1% v/v AB/AM and 0.3% w/v collagenase type II (Worthington). The cartilage was digested for 18hrs in an incubator at 37 °C and 5% CO_2.

The resulting cell suspension was poured through a 100 μm strainer and centrifuged to pellet the cells. The supernatant was removed and the cells were resuspended in DPBS with 1% v/v AB/AM. Centrifugation and resuspension was performed three times to completely rinse the cells. The final resuspension was in DMEM with 1% v/v AB/AM and 10% v/v fetal bovine serum (FBS, Gemini Bio-Products). The concentration and viability of the cell suspension was assessed with a hemocytometer and trypan blue.

A total of 50×10^6 cells were spun down and 1 mL of an alginate solution, prepared for ionic or covalent cross-linking as described above, was poured onto the cell pellet through a 0.8 μm syringe filter. The alginate and cells were gently aspirated to disperse the cells in the alginate. The suspension was then vortexed for no more than 15 s to homogenize the suspension. The alginate mixture was then ionically or covalently cross-linked as described above. Hydrogels were incubated at 37 °C in DMEM with 1% v/v AB/AM and 10% v/v FBS for 48 h. After 1−2 days, viability was assessed via calcein-AM and ethidium homodimer-1 staining (Live/Dead Kit, Invitrogen).[54] Hydrogels were incubated for 90 min in the dark at room temperature with 500 μL of 0.05 μM calcein-AM and 1 μM ethidium homodimer-1 in PBS. The hydrogels were then rinsed with PBS and immediately imaged using confocal microscopy. Viability was computed as the fraction of cells stained with calcein-AM but not ethidium homodimer-1. At least six hydrogel sections were sampled for each stain for a total of at least 3000 cells counted.

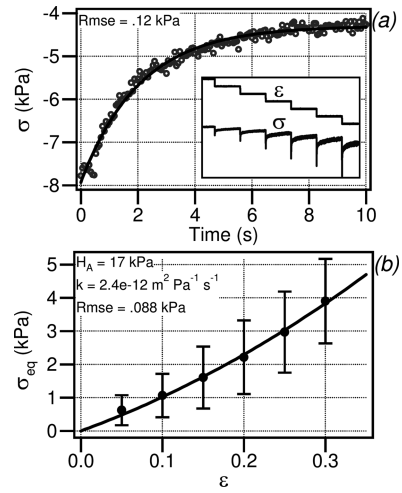

Figure 2. Stress relaxation tests performed on ionically cross-linked hydrogels. A series of step displacements produced stress responses that peaked and then decayed over time (a, inset). Each decay was fit by an exponential function (a), and the equilibrium stress followed a strain-stiffening constitutive relation (b). Bars are mean ± standard deviation for $n = 5$. Rmse is the root mean squared error of the model fit.

Statistics. Electromechanical properties were analyzed with one- or two-factor ANOVA using Tukey posthocs. The significance level for all cases was set at $\alpha = 0.05$.

3. Results

Experiments were conducted to investigate the use of ionic and covalent cross-linking of alginate in conjunction with silica microparticle doping as a means of decoupling flow-induced electric fields from the mechanical properties of hydrogel tissue scaffolds using biocompatible materials and fabrication techniques. Four types of alginate hydrogels were fabricated: (1) ionically cross-linked alginate, (2) ionically cross-linked alginate doped with silica microparticles, (3) covalently cross-linked alginate, and (4) covalently cross-linked alginate doped with silica microparticles. Stress relaxation and dynamic compression tests were performed in order to characterize the electromechanical properties of the hydrogels. Biocompatibility of ionically and covalently cross-linked hydrogels was assessed in a two-day viability assay of seeded primary bovine chondrocytes.

In stress relaxation tests, the hydrogels exhibited exponential relaxation consistent with poroelastic theory for the re-equilibration of fluid and solid within a poroelastic material after compression (Figure 2a), and the equilibrium stress−strain curves followed characteristic strain-stiffening behavior (Figure 2b). In dynamic compression, stress and streaming potential responded at the applied frequency (Figure 3a), with a sigmoidal frequency dependence characteristic of the transition between fluid-static and fluid-dynamic regimes (Figure 3b).

Ionically and covalently cross-linked alginate hydrogels had similar mechanical properties with low and high electrokinetic

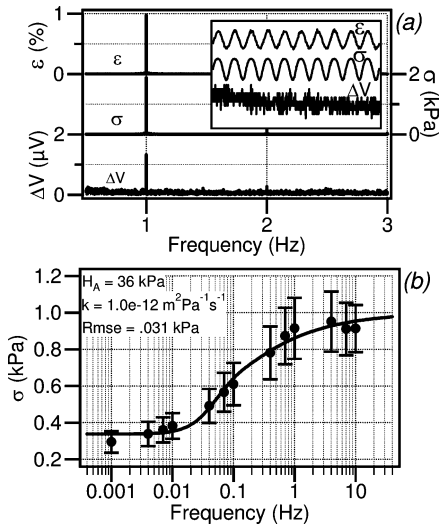

Figure 3. Dynamic compression tests performed on ionically cross-linked hydrogels. Dynamically applied strains produced oscillatory stress and streaming potential signals (a,inset), which were Fourier transformed to calculate the amplitude and phase of the signals (a). These signals showed frequency dependent behavior, which was fit to models for the dynamic electromechanical behavior of cartilage (b). Bars are mean ± standard deviation for $n = 5$. Rmse is the root mean squared error of the model fit.

coupling, respectively. The aggregate (equilibrium) modulus and permeability of the two types of hydrogels were similar (Figure 4b,c), while the electrokinetic coupling coefficient was about 3× greater in the covalently cross-linked hydrogels (Figure 4d; $p < 0.01$). Flow-induced streaming potentials were greater by a factor of 1.50 in the covalently cross-linked hydrogels ($p < 0.05$; Figure 4a).

The addition of silica microparticles led to a higher streaming potential in covalently cross-linked alginate, but a similar increase was not observed when silica was added to ionically cross-linked alginate (two-factor ANOVA, $p < 0.05$). The silica caused a 53% increase in the streaming potential of the covalently cross-linked hydrogels, which was in close proportion to the 62% increase in fixed charge density imparted by the addition of the silica (calculated from the density, surface area, and surface charge density of the silica particles). However, the streaming potential of the ionically cross-linked hydrogels increased by only 15% (Figure 4a), a difference that did not reject the null hypothesis for these samples.

Fabrication of ionically and covalently cross-linked hydrogels was biocompatible with primary bovine articular chondrocytes. The viability of chondrocytes seeded at a density of 50×10^6 cells/mL was assessed after incubation for 1−2 days. Total number of counted cells was 7000 and 3000 for ionically and covalently cross-linked hydrogels, respectively. The viability of chondrocytes seeded into ionically cross-linked gels was 84 ± 6%, and the viability of chondrocytes seeded into covalently cross-linked gels was 90 ± 2% ($n = 9$).

4. Discussion

The results demonstrate the ability to fabricate mechanically similar hydrogels with different electrokinetic coupling coefficients. Ionically cross-linked gels show relative insensitivity of streaming potential and electrokinetic coupling to the addition of charged dopants, while the electromechanical properties of covalently cross-linked gels can be tuned by such changes. The addition of silica did not substantially change the modulus or permeability of ionically or covalently cross-linked hydrogels

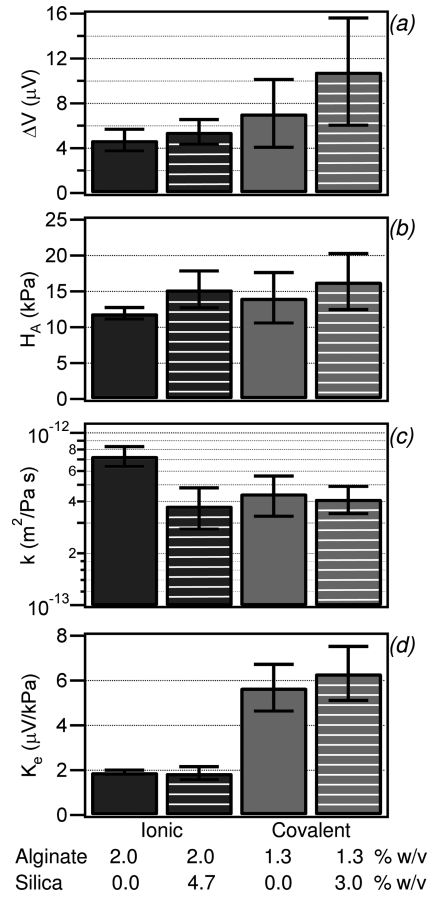

Figure 4. Mechanical and electrical properties of ionically and covalently cross-linked alginate hydrogels with and without silica. Ionically and covalently cross-linked hydrogels had similar modulus (b) and permeability (c), but streaming potentials (a) and the electrokinetic coupling coefficient (d) were different. Streaming potentials in ionically cross-linked hydrogels were not changed by the addition of negatively charged silica microparticles. In contrast, the streaming potentials in covalently cross-linked hydrogels were manipulated by adding negative charge. Bars are mean ± standard deviation for $n = 5$.

(Figure 4b,c), showing that microparticle doping can change the electrical properties of pairs of hydrogels while maintaining their mechanical similarity. The relatively minor change in modulus is consistent with theoretical predictions for low-volume-fraction inclusions.[55] The evidence suggests that the difference in the electrokinetic properties of ionically and covalently cross-linked hydrogels was due to a difference in net fixed charged density caused by the presence and absence of calcium, respectively. For each ionic cross-link, two negatively charged carboxyl groups on alginate chains were effectively canceled by the divalent calcium cross-linker,[56] whereas covalent cross-links left these negative charges free.[47] Consequently, streaming potentials of the ionically cross-linked hydrogels were lower than those of the covalently cross-linked hydrogels (Figure 4a), despite the fact that the ionically cross-linked hydrogels had a higher concentration of alginate and, thus, more charged groups. Furthermore, ionically cross-linked alginate exhibited little increase in streaming potential with the addition of silica, whereas covalently cross-linked alginate had an increase in streaming potential in close proportion to the increase in fixed charge density imparted by the silica (Figure 4a). This is consistent with model predictions, indicating that streaming potentials should increase proportionately with the increase in silica surface charge (or zeta potential).[57] Thus,

photo-cross-linking is critical primarily in that it allows perturbation of static charge in the hydrogel by eliminating charge-canceling divalent counterions. These results were consistent with the swelling properties of these gels. Relative changes in volume after equilibration were $-1.5 \pm 0.9\%$ for the ionically cross-linked gels and $136 \pm 17\%$ for the covalently cross-linked gels ($n = 5$), suggesting a Donnan effect was present only in the covalently cross-linked gels.

The techniques presented here for controlling the electromechanical properties of alginate hydrogels were developed with the critical constraint that they be compatible with seeding of primary cells. Well-established ionic cross-linking techniques were used for which the particular challenge is avoiding cell damage due to shear when mixing solutions. For covalent cross-linking, the obstacles to biocompatibility were DNA damage and photo-oxidation due to UV exposure, toxicity of the photoinitiator, and toxicity of the photoinitiator radicals. These problems were minimized by using a low toxicity photoinitiator (VA-086) that could still cross-link methacrylate groups at low UV exposure times. This photoinitiator's performance is notably different from the more commonly used Irgacure 2959 in that it creates a noncytotoxic radical upon photodissociation.[54]

The two-day viability results indicated that the fabrication techniques caused little damage to encapsulated chondrocytes. While additional work is necessary to verify the compatibility of these techniques with other cell types, this technique shows promise for the creation of viable scaffolds.

Mechanotransduction may be important for a variety of cells embedded in charged extracellular matrix, such as chondrocytes, osteocytes, tenocytes, and corneal fibroblasts. It has been demonstrated that enhanced chondrocyte biosynthesis of glycosaminoglycans occurs at certain frequencies and amplitudes of dynamically applied current,[58] as well as at locations where streaming potentials are high during dynamic compression.[39] These results indicate that chondrocytes may be responsive to electrical stimuli. Steps have been taken toward controlling streaming potentials by altering the fixed charge density of hydrogel systems,[59] but this has not been accomplished in a consistent mechanical environment, nor has it been accomplished in a biodegradable scaffold that may be used for tissue engineering. Because fluid transport and electric fields are coupled in single materials, developing suites of materials with decoupled properties creates new possibilities for studying these mechanotransduction processes.

5. Conclusion

Hydrogels were produced that had similar mechanical characteristics but different electrical characteristics, effectively decoupling these two properties. This was achieved by creating alginate hydrogels that were either ionically or covalently cross-linked. Ionic cross-linking, in which calcium binds negative charges on alginate polymers, effectively reduced the alginate charge density. Covalent cross-linking, on the other hand, left the charged groups on alginate unperturbed. This difference in fixed charge density gave rise to different streaming potentials.

Ionic and covalent cross-linking of alginate with microparticle doping was used to fabricate hydrogel tissue scaffolds with varying degrees of electrokinetic coupling. The biocompatibility of these techniques allows them to be implemented with seeded cells to study how a cell's electrokinetic environment affects its behavior. In particular, these techniques for the first time enable the effect of flow-induced electric fields on chondrocyte mechanotransduction to be studied independent of mechanical responses to dynamic compression. Such study will further understanding of chondrocyte mechanotransduction and instruct better design of tissue scaffold properties.

Acknowledgment. This work was supported by the Cornell Center for Materials Research. We thank J. P. Gleghorn for useful discussions.

References and Notes

(1) Vogel, K. G.; Heinegard, D. *J. Biol. Chem.* **1985**, *260*, 9298–9306.
(2) Olszta, M. J.; Cheng, X. G.; Jee, S. S.; Kumar, R.; Kim, Y. Y.; Kaufman, M. J.; Douglas, E. P.; Gower, L. B. *Mater. Sci. Eng., R* **2007**, *58*, 77–116.
(3) Handley, C. J.; Lowther, D. A.; McQuillan, D. J. *Cell Biol. Int. Rep.* **1985**, *9*, 753–782.
(4) Heinegard, D.; Oldberg, A. *FASEB J.* **1989**, *3*, 2042–2051.
(5) Kuettner, K. E.; Aydelotte, M. B.; Thonar, E. *J. Rheumatol.* **1991**, *18*, 46–48.
(6) Axelsson, I.; Heinegard, D. *Biochem. J.* **1975**, *145*, 491–500.
(7) Hassell, J. R.; Newsome, D. A.; Hascall, V. C. *J. Biol. Chem.* **1979**, *254*, 2346–2354.
(8) Wang, J. H.-C.; Thampatty, B. P.; Lin, J.-S.; Im, H.-J. *Gene* **2007**, *391*, 1–15.
(9) Vogel, V. *Annu. Rev. Biophys. Biomol. Struct.* **2006**, *35*, 459–488.
(10) Cho, M. R.; Thatte, H. S.; Silvia, M. T.; Golan, D. E. *FASEB J.* **1999**, *13*, 677–683.
(11) Hart, F. X. *Bioelectromagnetics* **2008**, *29*, 447–455.
(12) Seegers, J. C.; Engelbrecht, C. A.; van Papendorp, D. H. *Med. Hypotheses* **2001**, *57*, 224–230.
(13) Chenite, A.; Chaput, C.; Wang, D.; Combes, C.; Buschmann, M. D.; Hoemann, C. D.; Leroux, J. C.; Atkinson, B. L.; Binette, F.; Selmani, A. *Biomaterials* **2000**, *21*, 2155–2161.
(14) Berger, J.; Reist, M.; Mayer, J. M.; Felt, O.; Peppas, N. A.; Gurny, R. *Eur. J. Pharm. Biopharm.* **2004**, *57*, 19–34.
(15) Chang, S. C. N.; Tobias, G.; Roy, A. K.; Vacanti, C. A.; Bonassar, L. J. *Plast. Reconstr. Surg.* **2003**, *112*, 793–799.
(16) Grandolfo, M.; Dandrea, P.; Paoletti, S.; Martina, M.; Silvestrini, G.; Bonucci, E.; Vittur, F. *Calcif. Tissue Int.* **1993**, *52*, 42–48.
(17) Lee, C. R.; Grodzinsky, A. J.; Hsu, H. P.; Spector, M. *J. Orthop. Res.* **2003**, *21*, 272–281.
(18) Vaissiere, G.; Chevallay, B.; Herbage, D.; Damour, O. *Med. Biol. Eng. Comput.* **2000**, *38*, 205–210.
(19) Grassl, E. D.; Oegema, T. R.; Tranquillo, R. T. *J. Biomed. Mater. Res., Part A* **2003**, *66A*, 550–561.
(20) Bryant, S. J.; Anseth, K. S. *J. Biomed. Mater. Res., Part A* **2002**, *59*, 63–72.
(21) Yang, F.; Williams, C. G.; Wang, D. A.; Lee, H.; Manson, P. N.; Elisseeff, J. *Biomaterials* **2005**, *26*, 5991–5998.
(22) Pazzano, D.; Mercier, K. A.; Moran, J. M.; Fong, S. S.; DiBiasio, D. D.; Rulfs, J. X.; Kohles, S. S.; Bonassar, L. J. *Biotechnol. Prog.* **2000**, *16*, 893–896.
(23) Grodzinsky, A. J.; Lipshitz, H.; Glimcher, M. J. *Nature* **1978**, *275*, 448–450.
(24) Mow, V. C.; Kuei, S. C.; Lai, W. M.; Armstrong, C. G. *J. Biomech. Eng.* **1980**, *102*, 73–84.
(25) Lai, W. M.; Hou, J. S.; Mow, V. C. *J. Biomech. Eng.* **1991**, *113*, 245–258.
(26) Weinbaum, S.; Cowin, S. C.; Zeng, Y. *J. Biomech.* **1994**, *27*, 339–360.
(27) Wang, Q.; Zhong, S. Z.; Jun, O. Y.; Jiang, L. X.; Zhang, Z. K.; Xie, Y.; Luo, S. Q. *Clin. Orthop. Relat. R* **1998**, *348*, 259–268.
(28) Sharma, P.; Maffulli, N. *J. Bone Joint Surg. Am.* **2005**, *87A*, 187–202.
(29) Sisken, B. F.; Walker, J. Therapeutic Aspects of Electromagnetic Fields for Soft-Tissue Healing. In *Electromagnetic Fields: Biological Interactions and Mechanisms*; Blank, M., Ed.; American Chemical Society: Washington, DC, 1995; Vol. 250; pp 277−285.
(30) Kim, Y. J.; Bonassar, L. J.; Grodzinsky, A. J. *J. Biomech.* **1995**, *28*, 1055–1066.
(31) Bonassar, L. J.; Grodzinsky, A. J.; Frank, E. H.; Davila, S. G.; Bhaktav, N. R.; Trippel, S. B. *J. Orthop. Res.* **2001**, *19*, 11–17.
(32) Lee, C. R.; Grodzinsky, A. J.; Spector, A. *J. Biomed. Mater. Res., Part A* **2003**, *64A*, 560–569.
(33) Lee, C. R.; Grodzinsky, A. J.; Spector, M. *Tissue Eng.* **2003**, *9*, 27–36.
(34) Ragan, P. M.; Chin, V. I.; Hung, H. H. K.; Masuda, K.; Thonar, E.; Arner, E. C.; Grodzinsky, A. J.; Sandy, J. D. *Arch. Biochem. Biophys.* **2000**, *383*, 256–264.

(35) Grodzinsky, A. J.; Levenston, M. E.; Jin, M.; Frank, E. H. *Annu. Rev. Biomed. Eng.* **2000**, *2*, 691–713.
(36) Vunjak-Novakovic, G.; Martin, I.; Obradovic, B.; Treppo, S.; Grodzinsky, A. J.; Langer, R.; Freed, L. E. *J. Orthop. Res.* **1999**, *17*, 130–138.
(37) Kim, Y. J.; Grodzinsky, A. J.; Plaas, A. H. K. *Arch. Biochem. Biophys.* **1996**, *328*, 331–340.
(38) Buschmann, M. D.; Gluzband, Y. A.; Grodzinsky, A. J.; Hunziker, E. B. *J. Cell Sci.* **1995**, *108*, 1497–1508.
(39) Buschmann, M. D.; Kim, Y. J.; Wong, M.; Frank, E.; Hunziker, E. B.; Grodzinsky, A. J. *Arch. Biochem. Biophys.* **1999**, *366*, 1–7.
(40) Sun, D. Q.; Aydelotte, M. B.; Maldonado, B.; Kuettner, K. E.; Kimura, J. H. *J. Orthop. Res.* **1986**, *4*, 427–436.
(41) Bryant, S. J.; Bender, R. J.; Durand, K. L.; Anseth, K. S. *Biotechnol. Bioeng.* **2004**, *86*, 747–755.
(42) Burdick, J. A.; Anseth, K. S. *Biomaterials* **2002**, *23*, 4315–4323.
(43) Genes, N. G.; Rowley, J. A.; Mooney, D. J.; Bonassar, L. J. *Arch. Biochem. Biophys.* **2004**, *422*, 161–167.
(44) Gleghorn, J. P.; Jones, A. R. C.; Flannery, C. R.; Bonassar, L. J. *Eur. Cell Mater.* **2007**, *14*, 20–28.
(45) Hott, M. E.; Megerian, C. A.; Beane, R.; Bonassar, L. J. *Laryngoscope* **2004**, *114*, 1290–1295.
(46) Chang, S. C. N.; Rowley, J. A.; Tobias, G.; Genes, N. G.; Roy, A. K.; Mooney, D. J.; Vacanti, C. A.; Bonassar, L. J. *J. Biomed. Mater. Res., Part A* **2001**, *55*, 503–511.
(47) Smeds, K. A.; Grinstaff, M. W. *J. Biomed. Mater. Res., Part A* **2001**, *54*, 115–121.
(48) Li, Q.; Williams, C. G.; Sun, D. D. N.; Wang, J.; Leong, K.; Elisseeff, J. H. *J. Biomed. Mater. Res., Part A* **2004**, *68A*, 28–33.
(49) Kim, S. H.; Chu, C. C. *J. Biomed. Mater. Res., Part A* **1999**, *49*, 517–527.
(50) Carraher, C. E. *Seymour/Carraher's Polymer Chemistry*, 5th ed.; Marcel Dekker: New York, 2000.
(51) Quinn, T. M.; Grodzinsky, A. J. *Macromolecules* **1993**, *26*, 4332–4338.
(52) Frank, E. H.; Grodzinsky, A. J. *J. Biomech.* **1987**, *20*, 615–627.
(53) Frank, E. H.; Grodzinsky, A. J. *J. Biomech.* **1987**, *20*, 629–639.
(54) Rouillard, A. D.; Tsui, Y.; Polacheck, W. J.; Lee, J. Y.; Bonassar, L. J.; Kirby, B. J. *Tissue Eng., Part C* **2010**, submitted for publication.
(55) Chen, H.-S.; Acrivos, A. *Int. J. Solids Struct.* **1978**, *14*, 349–364.
(56) Fang, Y.; Al-Assaf, S.; Phillips, G. O.; Nishinari, K.; Funami, T.; Williams, P. A.; Li, L. *J. Phys. Chem. B* **2007**, *111*, 2456–2462.
(57) Hill, R. J. *J. Fluid Mech.* **2006**, *551*, 405–433.
(58) Macginitie, L. A.; Gluzband, Y. A.; Grodzinsky, A. J. *J. Orthop. Res.* **1994**, *12*, 151–160.
(59) Malmonge, S. M.; Arruda, A. C. *Artif. Organs* **2000**, *24*, 174−178.

BM1001312